https://erjm.journals.ekb.eg
ISSN: 1110-1180

DOI: ---------

ERJ
Engineering Research Journal
Faculty of Engineering
Menoufia University

Dielectric Response of Cr-Doped TiO_2 Nanoparticles: Effect of Doping Concentration and Annealing Temperature

Ragab A. Elsad [1,2], Elsayed M. Farag[2], Ibrahim E. Eldafatry[1,2]*, Shehab A. Mansour [1,2]

[1] *Advanced Materials/Solar Energy and Environmental Sustainability (AMSEES) Laboratory, Faculty of Engineering, Menoufia University, 32511 Shebin El-Kom, Egypt*
[2] *Basic Engineering Science Department, Faculty of Engineering, Menoufia University, Shebin El-Kom, Egypt*
* Corresponding author. *E-mail address*: ebrahimeldafatry@gmail.com

ABSTRACT
The combined effect of doping chromium (Cr) as well as annealing temperature on the dielectric spectroscopy performance of titanium (TiO_2) was investigated. Accordingly, two series of chromium doped titania samples with the form ($Ti_{1-x}Cr_xO_2$) where X=0-25 mol% were fabricated utilizing the hydrolysis method. The first series was used as-synthesized while the second series was used after annealing at 500 ℃ for 1h. The microstructure of both synthesized series was characterized by X-ray diffraction (XRD) and Brunauer-Emmett-Teller (BET). The (XRD) result confirms the formation of the amorphous characteristics of such pure and Cr-doped TiO_2 (as-synthesized) and crystalline characteristics of such pure and Cr - doped TiO_2 (annealed at 500 ℃ for 1h). The average crystallite size in second series (annealed at 500 ℃) as estimated by the Scherrer's equation varies in the range of ~12–30 nm on doping of Cr ions in TiO_2. The measured surface area of TiO_2 is decreased by Cr doping in first series (as-synthesized) while it is increased by Cr doping in second series (annealed at 500 ℃). The variation in both dielectric constant (ε'), and ac conductivity (σ_{ac}) as a function of applied frequency at different doping concentration of Cr were investigated. The measurements confirms that both ε' and σ_{ac} values of TiO_2were decreased with Cr doping in first series and increased with Cr doping in second series.

Keywords: TiO_2 , Dielectric constant, Ac conductivity, Cr doping, Hydrothermal method.

1. Introduction

Recently, Doped semiconductor materials have attracted growing attention because of unique characters in different application such as the catalytic, optical, and electrical application. Existence of many crystalline polymorphs and morphologies have a widely impact on the electrical and dielectric properties of semiconductor oxides [1-4]. The properties of semiconductor nanoparticles (NPs) have greatly dependent on its size, therefore size controlling during synthesization allows for the fabrication of novel materials which used in DRAMS and dielectric resonators (DR) [1, 5]. Semiconductor NPs such as TiO_2, ZnO and Fe_2O_3 were used as filler into insulating polymer as well as transformer oil to improve their dielectric performance [6-9]. $TiO_2$is one of the most significant semiconductors widely studied recently due to its many features such availability, chemical stability, nontoxicity, optical-electronic properties, low cost, and high photocatalytic properties [2, 10]. So, TiO_2 has been widely used in a various applications such as gas, temperature sensors, photocatalytic, photoelectric devices, and microelectronics [3, 4]. The main categories of the crystallographic polymorph phases of TiO_2 resulting from annealing temperature are anatase, rutile, and brookite. The most common phases of TiO_2 are anatase and rutile. Anatase forms at low temperatures, whereas rutile forms at higher temperatures and is thermodynamically stable[11]. According to literature survey, the dielectric polarization and electrical conductivity of TiO_2 were modified by metal doping [2, 3, 10]. The dielectric constant of Fe doped TiO_2 which synthesized by sol–gel route, were reported in frequency range of 20 Hz to 10 MHz in which the dielectric constant of pure TiO_2 was enhanced with Fe doping until 4% mole and then decreased for further Fe doping [4]. Neodymium doped TiO_2 NPs have been created in anatase phase by a low temperature hydrothermal

route and the dielectric constant of pure TiO_2 measured at room temperature was decreased with increase Nd doping [11]. The conductivity of TiO_2 NPs prepared in anatase phase by sol–gel process was decreased with increasing Ni doping [3]. Samarium-doped TiO_2 NPs have been synthesized using the low-temperature hydrothermal method where it is found the decreasing in both ε' and σ_{ac} of pure samples with Sm doping [2].

In the present study, two series of pure TiO_2 and three different mole concentrations of Cr-doped TiO_2 NPs were prepared by using hydrolysis method. The first series was used as-synthesized and second series was used after annealing at 500 ℃ for 1h. The dependence of dielectric properties of the investigated samples in both series on frequency was studied. Also, the influences of Cr concentrations on the dielectric properties of TiO_2 in both series are discussed.

2. Experimental

2.1 Materials

All of the used reagents were analytical grade and bought from Aldrich. Titanium tetra isopropoxide (TTIP) [$Ti(OC_3H_7)_4$, 97%] , chromium (III) acetate hydroxide, and ethanol (EtOH) were used for synthetization of Cr -doped TiO_2 NPs .

2.2 Synthesis of Cr - doped TiO_2 NPs

Pure TiO_2 and Cr -doped TiO_2 have been prepared by hydrolysis of TTIP in the existence of the required amount of chromium (III) acetate hydroxide reported elsewhere[12]. TTIP was hydrolysis in EtOH aqueous solution which prepared by mixing 3ml of distilled water and 97 ml of ethanol. For the undoped TiO_2 sample, 0.0125 mole of TTIP was added gradually into the prepared EtOH aqueous solution under stirring at room temperature (RT). While, for the Cr-doped TiO_2, the specified molar ratio of chromium (III) acetate hydroxide was dissolved in the prepared EtOH aqueous solution until a perfect solution was attained. Then, 0.0125 mole of TTIP was added slowly into such perfect solution under stirring at RT. The used molar percentage ratios between the chromium (III) acetate hydroxide to TTIP are 0, 5%, 15%, and 25%. The attained solutions for both pure TiO_2 and doped samples were stirred for another hour at the same condition. The acquired gels were saved 36 h in a closed beaker at RT to achieve hydrolyze TTIP and create mono-dispersed TiO_2 particles. Then, the aged gels were dried at 100 ℃ for 8 h to ensure the extraction of water and alcohol from the solution. The obtained fine powders with white color for pure TiO_2 and green color for Cr-doped TiO_2 are considered as-synthesized series. The second crystallite series was obtained by annealing (as- synthesized) samples at 500 ℃ for 1 h. The sets of first series (as-synthesized) samples and the second series (annealed 500 ℃ for 1 h) were used in the present study are labelled according to the used temperatures and doping as listed in Table 1.

Table1. The estimated crystallite sizes, surface area and rutile to anatase ratio of prepared nanocrystalline samples.

Sample		CrOAc Hydroxide %mol	Surface area (g^2m)	Crystallite (size (D, nm	Rutile phase %
1st Series (as-synthesized)	-S1100	0	447.337		
	S2-100	5	248.234		
	100-3S	15	45.5706		
	-4S100	25	9.41026		
2nd Series (annealed at 500°C)	S1-500	0	16.5536	12	5.26
	S2-500	5	71.4608	9.2	56.34
	500-3S	15	104.499	9.7	71
	4S-500	25	149.975	30.7	62.8

2.3 Characterization

The crystal structure of the Synthesis samples was obtained by using X-ray diffractometer of type Phillips X'pert (MPD3040) with a monochromatic CuKα (λ=1.5406 Å). The step-scan mode was selected as scanning mode to record the intensities of the diffracted X-rays with a step size of 0.03^O over range of 10^o to 80^o.

Brunauer-Emmett-Teller (BET) surface area measurements of the studied sets of samples were done using a Micromeritics Gemini 2375 nitrogen adsorption analyzer. The samples were exposed to degassing at 80 ℃ for 2 h under flowing nitrogen gas prior the measurement.

The dielectric parameters (ε' and σ_{ac}) of the investigated samples have been measured by dielectric spectroscopy using LCR bridge (Hioko 3532-50 Hi tester). To get the disk which used in measurements, the prepared powders have been pressed using a die with a diameter of 10 mm under 200 bar pressure. The obtained disk was coated at both sides with silver to achieve good contact during measurements. Moreover, each sample has been laid out between the electrodes under the same spring force and left at this condition for 2 h before the measurements. The LabVIEW-based software employed to measure 15 times of ε' and σ_{ac} at each frequency step during 5s and then records the average value.

2. Results and discussion

3.1 Microstructural characterization of synthesized pure and Cr -doped TiO_2 Samples

Phase purity, crystal phase identification, rutile to anatase ratio and crystallite size of synthesized samples were performed by utilization of X-ray diffraction technique. XRD patterns of pure and Cr - doped TiO_2, as synthesized are shown in Fig.1. For as-synthesized samples (S1-100, S2-100, S3-100 and S4-100), No distinctive diffraction lines are found in the diffraction pattern. But all samples have a clear step-hump that recognizes the amorphous characteristics of such pure and Cr- doped TiO_2 samples[12, 13].

XRD patterns of the pure and Cr - doped TiO_2, annealed at 500 ℃ are shown in Fig. 2. Such a figure reflects that diffraction lines of pure TiO_2 are well assigned to the anatase phase with the tetragonal structure on the basis of standard crystallographic data in JCPDS file no. 71-1166 [14] . while some diffraction lines assigned to the rutile phase are appeared by insertion Cr which means transformation from anatase to rutile. The XRD patterns of doped samples (S2-500, S3-500 and S4 -500) do not appear characteristic peak due to chromium oxide which refers to Cr remained as an amorphous phase without incorporating to TiO_2 lattice or travels to replacement sites in TiO_2. So the degree of crystalline is reduced by increasing Cr dopant due to the inhibiting of solidifying of particles during the annealing process[15] .

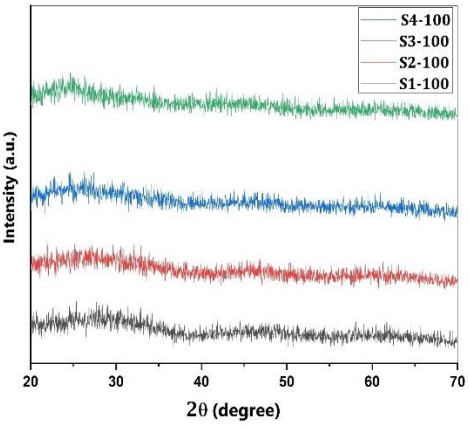

Fig.1 XRD pattern of as-synthesized samples (S1-100, S2-100, S3-100 and S4-100)

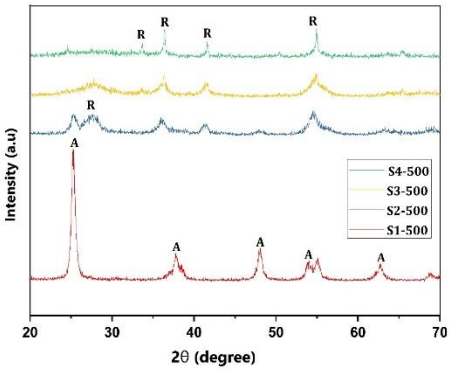

Fig.2 XRD pattern of Cr doped and pure TiO_2 samples annealed at 500 ℃ (S1-500, S2-500, S3 -500 and S4 -500), A: Anatase phase, R: Rutile phase

The average crystallite sizes (D) of the pure and Cr - doped TiO_2 samples annealed at 500 ℃ were estimated from all XRD peaks using eq (1) (Scherer's equation) and illustrated in Table 1[16]

$$D=0.9\lambda / (\beta \cos\theta) \quad (1)$$

where λ (0.154nm), β and θ are the X-ray wavelength, the full width at half maximum (FWHM) of the diffraction peak and the Bragg diffraction angle, respectively. The crystallite size of pure TiO_2, annealed at 500 ℃, was slightly decreased with Cr doping up to 15 mol % then it was enhanced again for Cr doping 25 mol %. The decrement in crystallite size with Cr doping up to 15 mol % can be attributed to a decrement in the intergranular contacts numbers through neighboring titanium grains because of existing Cr ions which act to inhibit the grain growth [17, 18] .

From eq (2), Rutile to anatase ratio were calculated using the relationship between the integrated intensities of anatase (1 0 1) peak and rutile (1 1 0) peak and illustrated in Table 1,

$$x= (1+0.8\ I_A/I_R)^{-1} \quad (2)$$

Where x is the rutile weight percentage in the powder sample, and I_A and I_R are the X-ray intensities of the anatase and rutile respectively [19]. The fundamental peak of the anatase phase in X-ray diffraction patterns is present at $2\theta=25.2^0$ assigned to the 101 planes (JCPDS 21-1272) and the fundamental peak of the rutile phase locates at $2\theta=27.4^0$ corresponding to its 110 planes (JCPDS 21-1276). The estimated ratio between rutile and anatase in Table 1 confirms the transformation from anatase to rutile by Cr doping. The results of BET showed that the surface area have a great dependency on Cr content. The results

showed a significant decrease in surface area from 447.3 (m^2 / g) for pure sample to 9.4 (m^2 / g) for doping sample with 25% mole in first Series (as-synthesized) as a result of decrease TOPV from 0.2645 to 0.010934 (cc/g) by Cr doping .In contrast, the second Series (annealed at 500 ℃) samples, the surface area increased from 16.5 (m^2 / g) to 149.97(m^2 / g) by Cr doping which can be explained by porous structure. Y.-S. Jung et al studied the effect of doping TiO_2 with Cr and found that the surface area of pure TiO_2 increased from 8 to 50 (m^2 / g) by doping with 30% Cr [20]. V S, Smitha et al and Xu, Guangqing et al reported that the surface area of pure TiO_2 increased with silica doping [21, 22].

3.2 Dielectric spectroscopic properties

3.2.1 Effect of frequency on dielectric parameters

Figure 3 shows the variation of dielectric constant (ε') of pure and Cr- doped TiO_2 samples (as-synthesized) as a function of the applied frequency in the range of 50 Hz to 10 MHz at RT. This figure reflects that the significant response of the dielectric constant to the applied frequency in which it has a high value at a low frequency and semi-constant at a high frequency. The high value of the dielectric constant at low-frequency intervals can be attributed to the existence of all sorts of polarization mechanisms such as space charge, dipolar, ionic, and electronic polarization [23, 24] .In fact, the polarization in nanomaterial's is arising mainly from space charge polarization, the hopping exchange of charge carriers between localized states, and the displacement of dipoles resulting from the applied field [2, 15]. In more specifically, most dipoles existing in the material do not have suitable time at high frequency to align with an external field, so the contribution of the orientation polarization is reduced. Also, the hopping exchange probability of charge carriers between localized states is increasing at a high frequency so the creation of space charge is restricted. Therefore, the contribution of space charge polarization at high frequency is reduced [25, 26]. It can be seen also from inset of Fig. 3 that the dielectric constant values were exhibited significant dependency on Cr concentration. The dielectric constant of pure TiO_2 is decreased by an increase of Cr doping due to interfacial charge transfer. Similar results have been shown for TiO_2 doped with different metal such as Fe, Nd, Sm and Al- doped [2, 4, 27, 28]. In more specifically, adding Cr to pure TiO_2 samples make the grain boundary thickener that leads to a decline in the polarization mechanism and hence of the dielectric constant (ε').

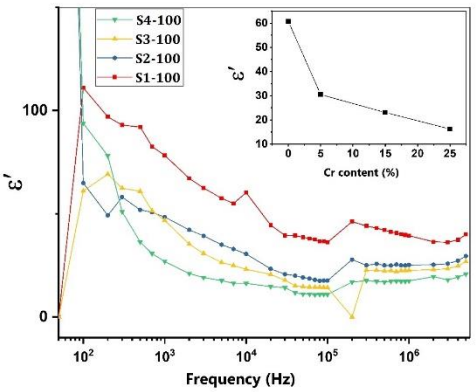

Fig.3 Variation of ε' of pure and Cr-doped TiO_2 samples (as synthesized) with applied frequency at RT. The inset represents the variation of dielectric constant with Cr content at 10 KHz

Variation of ε' with applied frequency field for pure and doped TiO_2 samples (annealed at 500 ℃) in the frequency range from 100 Hz to 10 MHz is shown in Fig. 4. The dielectric constant of all these investigated samples is decreased with applied field frequency increase in the frequency range from 50 Hz to 10 kHz and become semi-constant in the frequency range from 10 kHz to 5 MHz. This reduction in dielectric constant with increasing frequency is the normal behavior due to the weakness of the contribution of both orientation and space charge polarization at a high frequency. Typical values of dielectric constant at 10 kHz are 25, 30.5, 32.4, and 46 for 0.0, 5.0,15.0, and 25.0 mole% Cr-doped samples, respectively as shown in inset of Fig. 4.

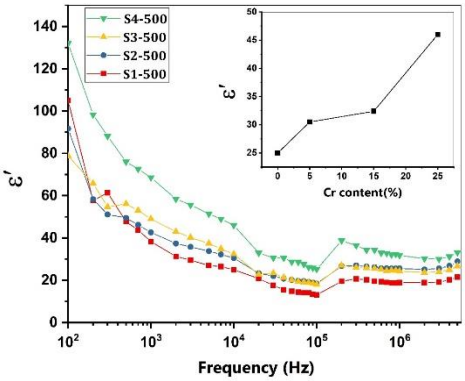

Fig.4 Variation of ε' of pure and Cr -doped TiO_2 samples (annealed at 500 ℃) with applied frequency at RT. The inset represents the variation of ε' with Cr content at 10 KHz

In contrast to the (as-synthesized) samples, the dielectric constant of TiO_2 is increased with increasing Cr doping that may be assigned to the difference in the oxidation state between pure and doped TiO_2 samples and indicates rotation in Ti^{+4}/Ti^{+3} ion pairs during annealing at 500 ℃. Consequently, the creation of oxygen vacancies in crystal lattice and thereby distortion in crystal structure are obtained[29] . This is considered as a source to produce the interchange of electrons in between the ions therefore it enhances the orientation polarization[10]. Moreover, the surface area per mass was found to increase with doping as shown in Table 1 subsequently, the number of OH groups attached to the particle surface increase so the dielectric constant increase with doping[4].

Figure 5 shows the variation of σ_{ac} of pure and doped TiO_2 samples (as synthesized) with applied frequency in range from 1000Hz to 5 MHz at RT. It was found that, σ_{ac} of investigated samples were almost independent on the frequency up to 100 kHz. Beyond this frequency, σ_{ac} values showed slight increment for doped samples and massive increment for pure TiO_2 with increasing applied frequency. The improvement in σ_{ac} at high frequencies approved the existence of the polaron hopping mechanism in the synthesized sample. In the high frequency region, the short-range intrawell hopping of charge carriers between localized states happened in a disordered method [28]. In more specifically, the creative force through the electric field helps to release trapped charges which were generated through the exchange interaction of various metal ions.

σ_{ac} is directly related to dielectric relaxation because of immobile charge carriers which follow the ac power-law formula [30, 31] ,eq (3).

$$\sigma_{ac} = k\,\omega^{m} \qquad (3)$$

where k is constant, ω is the angular frequency at which σ_{ac} was measured, and m is the exponent frequency which takes values between zero and one and depends on elements. The exponent frequency was estimated from the slope of graph between lnσ and ln ω as shown in fig.6. The typical values of the exponent frequency are 0.718, 0.699, 0.524, and 0.555 for (S1-100, S2 -100, S3-100 and S4-100) respectively which refers to reduction in the exponent frequency with Cr doping up to 15% mole of Cr doping, after this percentage the exponent frequency return to increase with Cr doping. The inset of Fig 5 also shows the effect of Cr doping on σ_{ac} of TiO_2 at frequencies 100 kHz and 1 MHz. Such a Figure reflects that the doping effect can be neglected at frequency of 100 kHz and exhibited a clear trend at 1MHz in which σ_{ac} of TiO_2 was decreased by Cr doping. At higher frequency, the reduction in σ_{ac} of pure TiO_2 by Cr doping can be attributed to decreasing the number of charge carriers involved in the doping mechanism where Cr ions effectively captured charge carriers [2, 28].

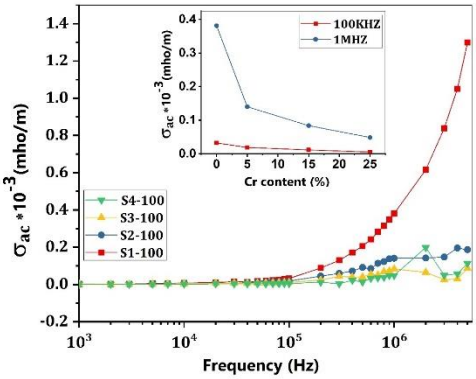

Fig.5 Variation of σ_{ac} of pure and Cr-doped TiO_2 samples (as synthesized) with applied frequency at RT. The inset represents the variation of σ_{ac} with Cr content at 100 KHz and 1 MHz

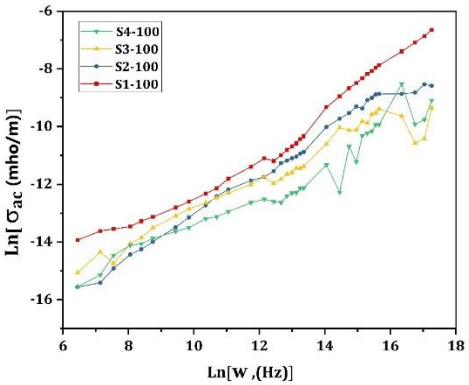

Fig.6 Variation of ln σ_{ac} of pure and Cr-doped TiO_2 samples (as synthesized) with ln(ω) at RT.

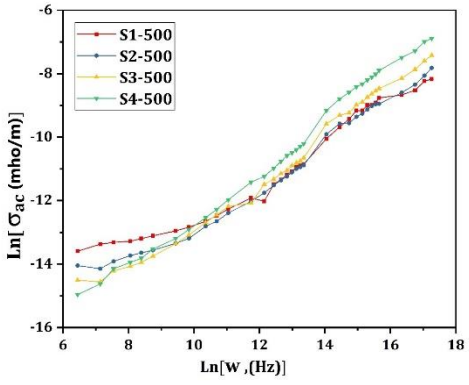

Fig .7 Variation of ln σ_{ac} of pure and Cr-doped TiO_2 samples (annealed at 500 ℃)) with ln(ω) at RT.

Fig .7 shows the variation of ln σ_{ac} of pure and Cr - doped TiO_2 samples (annealed at 500 ℃) with ln(ω) at RT. The typical values of the exponent frequency are 0.57, 0.636, 0.719, and 0.789 for S1-500, S2-500, S3-500, and S4-500 respectively which refers to enhancement in the exponent frequency with Cr doping. Figure 8 shows the variation of σ_{ac} of pure and Cr-doped TiO_2 samples (annealed at 500 ℃) as a function of frequency range from 1KHz to 10MHz at room temperature. The σ_{ac} of all samples almost constant up to 100 kHz and then enhanced steeply thereafter. The inset of Fig 8 represents the dependency of σ_{ac} on Cr doping at frequencies 200 kHz and 3 MHz. Unlike as synthesized samples, it was found at high frequency that the σ_{ac} of TiO_2 was increased by Cr doping. This enhancement in AC behavior can be attributed to the enhancement in hopping of charge carriers or diverse ionic states of Cr and Ti ions. Therefore, it causes a variation in charges that is responsible for the creation of oxygen vacancies and crystal defects in the TiO_2 lattice to preserve the charge neutrality [10, 32] . This may be resulted from the existence of a small polaron hopping mechanism [33]. By increasing Cr concentration TiO_2, the production of oxygen vacancies will improve which increase the hopping in the system.

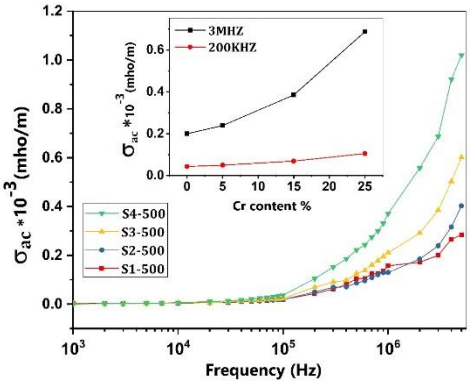

Fig.8 Variation of σ_{ac} of pure and Cr- doped TiO_2 samples (annealed at 500 ℃) with applied frequency at RT. The inset represents the variation of σ_{ac} with Cr content at 200 KHz and 3 MHz

4. Conclusion

In this work, the physical, and dielectric spectroscopy of fabricated pure and Cr- doped TiO_2 nanoparticles were investigated as-synthesized as well as after annealing at 500 ℃. XRD results revealed that the amorphous characteristics of such pure and Cr - doped TiO_2 samples in first series as synthesized while crystalline characteristics of such pure and Cr-doped TiO_2 samples annealed at 500 ℃. in second series. Also, some rutile peaks are appeared in annealed sample by Cr doping referring to change from anatase to rutile. The surface area of TiO_2 was decreased by Cr doping in first series while it was enhanced by Cr doping in second series. The response of both dielectric constant and σ_{ac} to applied frequency is obvious for all investigated samples. By increase Cr doping, dielectric constant is decreased in first series and enhanced in second series. Also, the dependency of exponent frequency on Cr doping is decreased in first series but enhanced in second series.

5. References

[1] A. K. Abdul Gafoor, M. M. Musthafa, K. Pradeep Kumar, and P. P. Pradyumnan, "Effect of Ag doping on structural, electrical and dielectric properties of TiO_2 nanoparticles synthesized by a low temperature hydrothermal method," Journal of Materials Science: Materials in Electronics, vol. 23, pp. 2011-2016, 2012.

[2] A. K. Abdul Gafoor, J. Thomas, M. M. Musthafa, and P. P. Pradyumnan, "Effects of Sm^{3+} Doping on Dielectric Properties of Anatase TiO_2 Nanoparticles Synthesized by a Low-Temperature Hydrothermal Method," Journal of Electronic Materials, vol. 40, p. 2152, 2011.

[3] K. Krishnan, K. Pandian, and N. Jaya, "Effect of nickel doping on structural, optical and electrical properties of TiO_2 nanoparticles by sol–gel method" Applied Surface Science vol. 256, pp. 6829-6833, 2010.

[4] D. Singh , P. Yadav , N. Singh , C. Kant , M. Kumar , S. D. Sharma & K. K. Saini, "Dielectric properties of Fe-doped TiO_2 nanoparticles synthesised by sol–gel route," Journal of Experimental Nanoscience - J EXP NANOSCI, vol. 8, pp. 1-13, 2011.

[5] P. Padmini, T. R. Taylor, M. J. Lefevre, A. S. Nagra, R. A. York, and J. S. Speck, "Realization of high tunability barium strontium titanate thin films by rf magnetron sputtering," Applied Physics Letters, vol. 75, pp. 3186-3188, 1999.

[6] S. A. Mansour, R. A. Elsad, and M. A. Izzularab, "Dielectric properties enhancement of PVC nanodielectrics based on synthesized ZnO nanoparticles," Journal of Polymer Research, vol. 23, p. 85, 2016.

[7] R. A. Elsad, S. A. Mansour, and M. A. Izzularab, "Loading different sizes of titania

nanoparticles into transformer oil: A study on the dielectric behavior," Journal of Sol-Gel Science and Technology, vol. 93, pp. 615-622, 2020.

[8] S. A. Mansour, R. A. Elsad, and M. A. Izzularab, "Dielectric spectroscopic analysis of polyvinyl chloride nanocomposites loaded with Fe2O3 nanocrystals," Polymers for Advanced Technologies, vol. 29, pp. 2477-2485, 2018.

[9] M. M. Habashy, A. M. Abd-Elhady, R. A. Elsad, and M. A. Izzularab, "Performance of PVC/SiO_2 nanocomposites under thermal ageing," Applied Nanoscience, vol. 11, pp. 2143-2151, 2021.

[10] M. Abushad, M. Arshad, S. Naseem, S. Husain, and W. Khan, "Role of Cr doping in tuning the optical and dielectric properties of TiO_2 nanostructures," Materials Chemistry and Physics, vol. 256, p. 123641, 2020.

[11] J. Kim, D.-W. Kim, H. Jung, and K. Hong, "Influence of Anatase-Rutile Phase Transformation on Dielectric Properties of Sol-Gel Derived TiO_2 Thin Films," Japanese Journal of Applied Physics, vol. 44, pp. 6148-6151, 2005.

[12] J. Yu, W. Ho, and L. Zhang, "Preparation of Highly Photocatalytic Active Nano-Sized TiO_2 Particles Via Ultrasonic Irradiation," Chemical communications (Cambridge, England), vol. 2001, pp. 1942-3, 2001.

[13] S. Mansour, "Non-isothermal crystallization kinetics of nano-sized amorphous TiO_2 prepared by facile sonochemical hydrolysis route," Ceramics International, vol. 45, 2018.

[14] F. H. Alkallas, T. A. Al-Rebdi, and S. A. Mansour, "Structural and diffuse reflectance investigation of dysprosium-doped TiO_2 nanopowder synthesized by sonochemical hydrolysis technique," Physica B: Condensed Matter, vol. 603, p. 412664, 2021.

[15] S. Ghasemi, S. Rahimnejad, S. Rahman Setayesh, S. Rouhani, and M. Gholami, "Transition metal ions effect on the properties and photocatalytic activity of nanocrystalline TiO_2 prepared in an ionic liquid," Journal of hazardous materials, vol. 172, pp. 1573-8, 2009.

[16] K. Ocakoglu, S. A. Mansour, S. Yildirimcan, A. A. Al-Ghamdi, F. El-Tantawy, and F. Yakuphanoglu, "Microwave-assisted hydrothermal synthesis and characterization of ZnO nanorods," Spectrochimica Acta Part A: Molecular and Biomolecular Spectroscopy, vol. 148, pp. 362-368, 2015.

[17] P. Nair, J. Engell, J. Kumar, K. Keizer, T. Okubo, and M. Sadakata, "Pore-Structure Stabilization by Controlling the Particle Coordination," Journal of Materials Science Letters, vol. 14, pp. 1784-1788, 1995.

[18] P. Nair, F. Mizukami, T. Okubo, J. Nair, K. Keizer, and A. J. Burggraaf, "High-temperature catalyst supports and ceramic membranes: Metastability and particle packing," AIChE Journal, vol. 43, pp. 2710-2714, 1997.

[19] R. A. Spurr and H. Myers, "Quantitative Analysis of Anatase-Rutile Mixtures with an X-Ray Diffractometer," Analytical Chemistry, vol. 29, pp. 760-762, 1957.

[20] Y.-S. Jung, K.-H. Kim, T.-Y. Jang, Y. Tak, and S.-H. Baeck, "Enhancement of photocatalytic properties of Cr_2O_3–TiO_2 mixed oxides prepared by sol–gel method," Current Applied Physics - CURR APPL PHYS, vol. 11, pp. 358-361, 2011.

[21] S. V S, K. Manjumol, B. Vijayan, D. Ghosh, P. Perumal, and K. Warrier, "Sol–gel route to synthesize titania-silica nano precursors for photoactive particulates and coatings," Journal of Sol-Gel Science and Technology, vol. 54, pp. 203-211, 2010.

[22] G. Xu, Z. Zheng, Y. Wu, and N. Feng, "Effect of Silica on the Microstructure and Photocatalytic Properties of Titania," Ceramics International, vol. 35, pp. 1-5, 2009.

[23] O. F. El-Menshawy, A. R. EL-Sissy, M. S. El-wazery, and R. A. Elsad, "Electrical and Mechanical Performance of Hybrid and Non-hybrid Composites," International Journal of Engineering, vol. 32, pp. 580-586, 2019.

[24] S. F. A. Ali, R. A. Elsad, and S. A. Mansour, "Enhancing the dielectric properties of compatibilized high-density polyethylene/calcium carbonate nanocomposites using high-density polyethylene-g-maleic anhydride," Polymer Bulletin, vol. 78, pp. 1393-1405, 2021.

[25] R. A. Elsad, A. M. Abdel-Aziz, E. M. Ahmed, Y. S. Rammah, F. I. El-Agawany, and M. S. Shams, "FT-IR, ultrasonic and dielectric characteristics of neodymium (III)/ erbium (III) lead-borate glasses: experimental studies," Journal of Materials Research and Technology, vol. 13, pp. 1363-1373, 2021.

[26] M. Shams, Y. Rammah, F. El-Agawany, and R. Elsad, "Synthesis, structure, physical, dielectric characteristics, and gamma-ray shielding competences of novel P_2O_5–Li_2O–ZnO–CdO glasses," Journal of Materials Science: Materials in Electronics, vol. 32, pp. 1-11, 2021.

[27] A. T. Raghavender and K. Jadhav, "Dielectric properties of Al-substituted Co ferrite nanoparticles," Bulletin of Materials Science, vol. 32, pp. 575-578, 2009.

[28] A. Gafoor, M. Musthafa, and P. P. Pradyumnan, "Effect of Nd^{3+} Doping on Optical and Dielectric Properties of TiO_2 Nanoparticles Synthesized by a Low Temperature Hydrothermal Method," Journal of Nanoscience and Nanotechnology ,vol. 1, pp. 53-57, 2013.

[29] A. M. Abdel-Aziz, R. A. Elsad, E. M. Ahmed, Y. S. Rammah, F. I. El-Agawany, and M. S. Shams, "Physical, FTIR, ultrasonic, and dielectric characteristics of calcium lead-borate glasses mixed by Nd_2O_3/Er_2O_3 rare earths: experimental study," Journal of Materials Science: Materials in Electronics, vol. 32, pp. 19966-19979, 2021.

[30] R. T subramaniam and A. K. Arof, "Ionic conductivity studies of plasticized poly(vinyl chloride) polymer electrolytes," Materials Science and Engineering: B, vol. 85, pp. 11-15, 2001.

[31] H. M. Zaki, "AC conductivity and frequency dependence of the dielectric properties for copper doped magnetite," Physica B: Condensed Matter, vol. 363, pp. 232-244, 2005.

[32] I. G. Austin and N. F. Mott, "Polarons in crystalline and non-crystalline materials," Advances in Physics, vol. 18, pp. 41-102, 1969.

[33] A. K. Jonscher, "A new understanding of the dielectric relaxation of solids," Journal of Materials Science, vol. 16, pp. 2037-2060, 1981.